

## LARGE-SCALE IN-SITU FRACTURE OF ICE

J. P. Dempsey, R. M. Adamson and S. V. Mulmule  
Department of Civil and Environmental Engineering  
Clarkson University  
Potsdam, New York

### Abstract

Do the fracture properties at large scale differ significantly from those at small scale? Can laboratory-scale testing be used to predict properties at large scale? What particular problems are faced with large scale testing? How useful are the size-effect theories developed to date? The answers to these questions are key to the applicability of fracture mechanics in the fields of ice engineering, concrete design and rock mechanics.

### 1 Introduction

Early investigations involving the fracture of ice (and other quasi-brittle materials such as concrete and rock) assumed the validity of linear-elastic fracture mechanics (LEFM) for the laboratory specimens employed, and LEFM toughness parameters such as  $K_{1c}$  were determined. However, parameters such as  $K_{1c}$  and  $G_{1c}$  obtained from normal laboratory sized specimens were found to be dependent on the specimen size (Dempsey, 1991; Dempsey et al., 1992).

There was reason to believe that much larger specimens than first expected were required to obtain the  $K_{Ic}$  or  $G_{Ic}$  values. This necessitated the study of fracturing at larger scales.

The field trips (Table 1) were aimed at studying size effects in ice. Following is a brief summary of the experiments conducted on each trip. A detailed analysis of the applicability of existing size effect laws to the Phase II results is also provided.

Table 1: Large-Scale Tests in Alberta and Resolute

Date	Ice Type & Grain Size	Ice Th'ness h(m)	Test Geometries	Size L(m)	Scale	# Tests
1/15-29, 1992 Canmore, Alberta	S1 freshwater ice vertical c-axis $\approx 200$ mm	0.50	3pt <sup>a</sup> - FR <sup>b</sup> RT <sup>c</sup> - FR	0.50 0.34-28.64	1:81	4 9
4/17 - 5/7 1993 Resolute, N.W.T.	FY <sup>d</sup> sea ice slightly aligned $\approx 15$ mm	1.8	3pt - FR SQ <sup>e</sup> - FR SQ - FL <sup>f</sup>	3.0 0.5-80 3.0	1:160	1 15 2

<sup>a</sup>3pt - Three point bend; <sup>b</sup>FR - Fracture; <sup>c</sup>RT - Reverse-tapered base-edge-cracked

<sup>d</sup>FY - First Year; <sup>e</sup>SQ - Square Plate (L×L); <sup>f</sup>FL - Flexure

## 2 Phase I: Canmore, Alberta

The primary goal of Phase I was to assess the feasibility of large-scale, full-thickness ice fracture measurements. Other objectives included: (1) Field experimentation of specimen cutting and scribing, loading systems, servo-control and instrumentation; (2) Determination of fracture toughness of full-thickness freshwater ice, global elastic modulus and scale effects.

Due to the difficulties encountered in preparing the notched bend tests (Figure 1a), the reversed-taper geometry (RT) was adopted (Figure 1b) (DeFranco and Dempsey, 1994; Dempsey et. al, 1995). Nine RT tests, some with multiple loadings, yielded a scale range of 1:81 and included the then largest known controlled fracture test specimen ( $40.5 \times 40.5 \times 0.57$ m). A comparison of the maximum nominal stress and size was completed. Although there was a decreasing trend in maximum nominal stress with size, efforts to fit any sort of size effect law proved fruitless. This indicated the presence of other size effects due in a large part to the very large grain

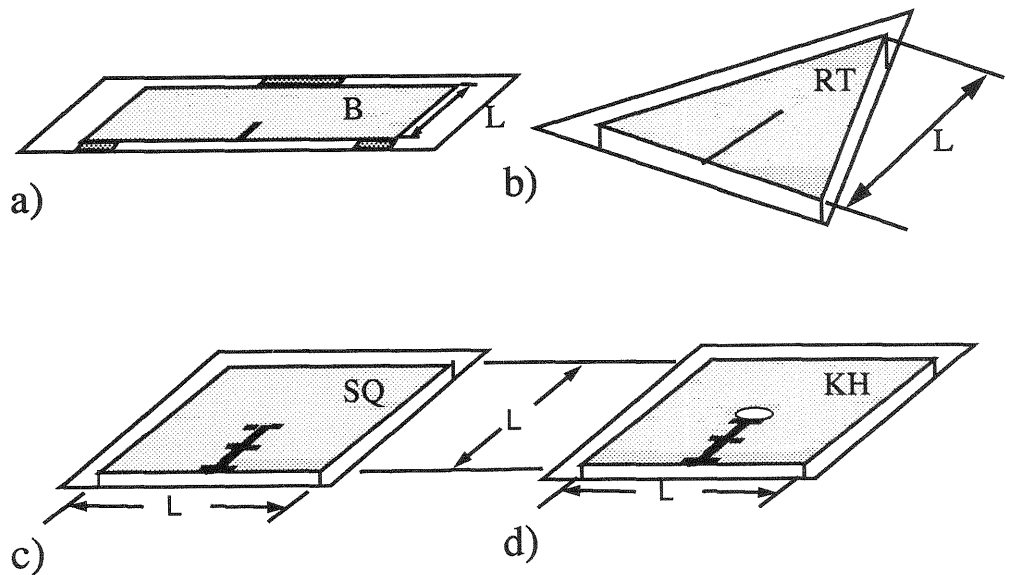


Figure 1: Test geometries: a) Three-point-bend fracture test, b) Reversed-taper geometry, c) Square plate, d) Square keyhole geometry

size. Details of this work can be found in Mulmule et al (1995).

### 3 Phase II: Resolute Bay, N.W.T.

Based on the success of Phase 1, large-scale fracture tests in full-thickness sea ice were conducted on Phase 2 in April, 1993 near Resolute, Northwest Territories. The tests in Resolute focused on the square plate geometry (Figure 1c, 1d), with the successful completion of fifteen fracture and three flexure tests—see Table 2 and Adamson et al (1995).

**Square Plate Experiments:** The square plates tested (Figure 1c) ranged from  $(0.5 \times 0.5 \times 1.8\text{m})$  to  $(80 \times 80 \times 1.8\text{m})$  covering a size range of 1:160. For each of these experiments, at least two crack opening displacements, the crack mouth and crack tip, were recorded. Typically, on the larger sizes where space permitted, crack openings were also recorded at intermediate points, referred to as the COD and NCTOD. Calculations of the initial modulus as computed from the CMOD and COD results are shown in Table 2.

**Flexure Experiments:** The testing of in-situ flexure beams proved to be a difficult task in Phase I. Test specimens using self-equilibrated loading (the RT on Phase I and the square plate on Phase II) were inherently easier to setup, requiring minimal preparation. This pro-

Table 2: Large Scale Ice Experiments @ Resolute Bay

Test ID	Length (m)	Crack Length (m)	$E_{COD}$ GPa	$E_{CMOD}$ GPa	$\bar{K}$ kPa $\sqrt{m}/s$	CTOD <sub>f</sub> $\mu m$	Control	Air Temp. °C
SQ1	1.0	0.3		8.2	0.48	6.5	Load	-9
SQ2	0.9	0.28		7.0	0.42		Load	-13
SQ3	10.0	3.0			0.45		Load	-13
SQ4	10.0	5.02	6.1	6.8	0.32		Load	-13
SQ5	30.0	9.0	5.0	7.0	0.21	40	Load	-13
SQ6	30.0	9.0	5.2	6.4	0.22	35	Load	-14
SQ7	30.0	9.0	11.5	8.7	0.46	35	Load	-15
SQ8	3.0	0.9	7.6	8.0	0.4	36	Load	-15
SQ9	3.0	0.9	5.2	5.8	5.14	45	CMOD	-3
SQ10	0.5	0.26		2.0	220	9	Load	-3
SQ11	30.0	9.0		2.0	1944	14	NCTOD	-14
SQ12	0.5	0.25		4.0	0.26	12	CMOD	-14
SQ13	80.0	24.0	3.9	4.7	0.17	39	Load	-12
SQ14	30.0	9.0			8.33		NCTOD	-12
SQ15	3.0	0.9			15		CMOD	-17
FL1	1.0	no crack					Load	-17
KH1	3.0	1.5					Load	-6
KH2	3.0	1.5					Load	-6

voiced the use of the square plate keyhole geometry (Figure 1d). This was a flexure test similar to the square plate fracture tests, except that a 20cm hole was bored at the crack tip. The displacement gauges were placed at points on the crack, similar to the fracture tests.

#### 4 Analysis of Size Effect Laws

In the case of concrete, to account for dissimilar initial cracks and a residual strength independent of size, modifications to the Bazant's size effect law (Bazant, 1984) were proposed by Kim et al (1993)—(from hereon called the KSL law). Carpinteri et al (1993) proposed a multifractal scaling law (MFSL) for similar reasons. However, if the size effect in a particular size range is desired, what actual size range needs to be tested to determine the associated size effect parameters? How do the parameters of various size effect laws change due to changes in the absolute size of specimen? Phrased differently, if a 1:10 test size range spans 0.5 m to 5 m, as opposed to

Table 3: Size Effect Laws

FIT	RANGE (m)	LAW	A MPa	B (m)	C	D MPa
FIT1	0.5–80	BZ	0.446	0.70	-	-
		MBZ	0.417	1.18	0.5892	-
		MKSL	0.367	2.34	1.037	0.039
		MFSL	-	1.46	-	0.050
FIT2	0.5–3	BZ	0.450	0.68	-	-
		MBZ	0.394	27957.13	7568.0	-
		KSL	-	-	-	-
		MFSL	-	0.57	-	0.125
FIT3	3–80	BZ	0.241	2.71	-	-
		MBZ	-	-	-	-
		KSL	0.261	2.26	0.5	-0.002
		MFSL	-	1.78	-	0.038
FIT4	0.9–80	BZ	13.881	0.00055	-	-
		MBZ	7.020	0.00208	0.497	-
		KSL	8.218	0.00151	0.5	0.004
		MFSL	-	2.26	-	0.024
FIT5	3–30	BZ	0.242	2.66	-	-
		KSL	0.252	3.35	0.5	-0.015
		MFSL	-	1.67	-	0.042

the test range 3 m to 30 m, how much do the size effect parameters differ?

The BZ, MFL and KSL size effect laws are now analyzed ( $\sigma_n$  represents the nominal maximum stress):

$$\sigma_n = \frac{A}{(1 + L/B)^{1/2}} \quad \text{BZ} \quad (1)$$

$$\sigma_n = D(1 + 10^B/L)^{1/2} \quad \text{MFSL} \quad (2)$$

$$\sigma_n = \frac{A}{(1 + L/B)^{1/2}} + D \quad \text{KSL} \quad (3)$$

In this paper, to ascertain if the exponents that are equal to 1/2 in the BZ law (5) and in the KSL law (7) are truly optimal, slight modifications were proposed. That is, the exponent was left unspecified prior to obtaining the best fit with experimental data. With the exponent set equal to  $C$ , the latter two laws are renamed as the MBZ and the MKSL laws:

$$\sigma_n = \frac{A}{(1 + L/B)^C} \quad \text{MBZ} \quad (4)$$

$$\sigma_n = \frac{A}{(1 + L/B)^C} + D \quad \text{MKSL} \quad (5)$$

The undetermined constants in each of the above laws,  $A$ ,  $B$ ,  $C$  and  $D$ , were obtained via precise curve fitting of the original size effect data from Phase II using TableCurve (an automated non-linear curve fitting program that uses a 64-bit Levenburg-Marquardt algorithm). It should be noted that while carrying out the linear regression for the BZ law according to the procedure given in RILEM draft recommendations (1991) it was noticed that the coefficient of variation of the intercept exceeded the prescribed limit of 0.20. The non-linear Levenburg-Marquardt algorithm obtained optimum fits.

Note that the constant  $A$  represents a small-scale strength value and is closely related to the tensile strength. For the BZ, MBZ, KSL and MKSL laws,  $B$  represents the ductile-brittle transition size, where this point lies at the intersection of the strength and LEFM asymptotes. The transitional size for the MFSL law is again given by  $B$ ; however, this point now apparently separates the disordered regime from the ordered (homogeneous) regime asymptotes. In the MBZ and MKSL,  $C$  represents an arbitrary exponent, to be found by a best fit of the data. The constant  $D$  represents the residual or size independent strength asymptote for very large sizes.

The smallest specimen had a dimension of 0.5 m while the largest specimen had a dimension of 80 m. To study this size range the results are divided in five different cases, as shown in Table 3.

FIT1 covers the complete size range of the data. The associated comparison of the experimental data and size effect law fits are shown in Figure 2a. Note that all of the size effect laws span the data with similar accuracy. The MFSL law tends to infinity for smaller specimen sizes. Both the MFSL and KSL laws tend to a constant maximum nominal stress (given by the value of  $D$ ) for very large sizes but they differ in the prediction of that value. The optimum value of the exponent for the MBZ law is slightly greater than 1/2 and the ductile to brittle transition size given by constant the constant  $B$  is slightly larger than 1 m.

FIT2 and FIT3 have been formulated to represent the sub-ranges of the data at the very low size range (spanning a 1:6 size range) and over the high size range (spanning a 1:27 size range), respectively. Attempts to find an optimum exponent for the MBZ law were not so successful. The KSL law could not be obtained for FIT2 and gave a negative constant stress for FIT3. The MFSL fit was good in FIT3. Graphical comparisons with the experimental data for FIT2 and FIT3 is provided in Figure 2b & 2c, respectively. FIT4 tried to judge the importance of the small scale data by removing the smallest sized specimen. FIT5 spans the middle part of the size

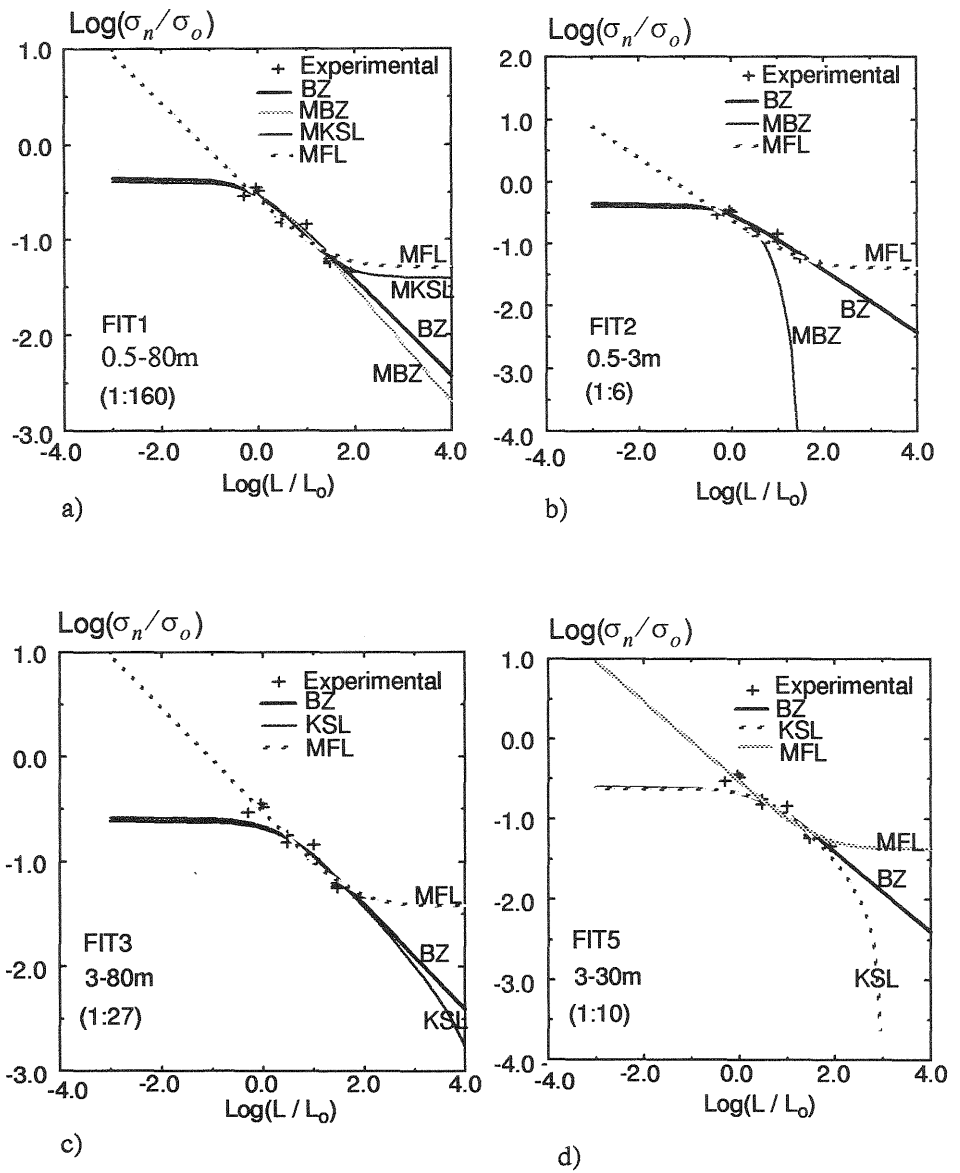


Figure 2: Comparison of various size effect laws:  $L_o \equiv 1$  m;  $\sigma_o \equiv 1$  MPa.

range by removing the data for both the small sizes as well as the largest size.

The MFSL law always overestimates the nominal maximum stress for small sizes because of its mathematical structure. Because of this inherent feature, removal of the data for smaller sizes has little effect as can be seen from FIT1, FIT3 and FIT5. The residual strength for the MFSL law is, however, very much affected by the cut off size chosen at the larger end. For FIT2, which has data provided up to sizes of 3 m, the residual strength predicted is much higher than the other fits for which either 30 m or 80 m is chosen as the data cut off. The difference in residual strength for 30 m and 80 m is much less but it is still difficult to say if (i) an asymptotic limit has been reached, or (ii) whether the concept of a residual strength at very large sizes is tenable.

The KSL law tries to combine the features of the BZ law for small sizes and features of the MFSL law for large sizes. For this reason, the KSL law performs well only when the data for very small and very large sizes are both included, as in FIT1. Exclusion of the data from either extremity lessens the accuracy of the prediction at the corresponding extremity as is seen from FIT3 and FIT5. If the size range is too small, it is not possible to fit the KSL law, as is the case in FIT2.

Similar considerations explain the results for the BZ law. The constant A, is governed by the smaller sized test data, as is apparent from comparing FIT1 & FIT2 with FIT3 & FIT5. Additionally, the smaller sized test data exerts a considerable influence on the predicted transition size as given by the constant B. If test results near the transition size are included, then the the size effect law accurately models the portion during which rapid changes occur and predictions for larger size ranges are good. Comparison of FIT1 and FIT2 where the input size range is reduced from 1:160 to 1:6 makes this point. However, if this 1:6 region is excluded, as has been done in FIT3 and FIT5, the effect on the parameters is considerable.

In FIT1, the optimum MBZ exponent for the complete size range is slightly different from  $1/2$  and the corresponding transition size is slightly larger. The optimum index, however may not always lead to correct behavior if tried on too small a size range as can be seen from MBZ in FIT2 as well as the fact that the MKSL law had to be abandoned in FIT3, FIT4 and FIT5. For materials like ice, where at the smaller sizes other effects like ploycrystallinity become important, scatter in the data is expected. Since the size effect laws like the BZ and KSL laws factor in a size effect due solely to crack and process zone size vs (homogeneous) specimen size, they are very sensitive to this scatter as can be seen from FIT4 where the 0.5 m



data was excluded. The latter observation indicates that a certain minimum size (relative to the average grain size) is necessary in order to obtain consistent results.

## 5 Conclusions

Preliminary analyses for the large-scale fracture tests from Phase I and Phase II are presented. The grain size has significant influence on the fracture of S1 freshwater ice. For Phase II, the predictive capability of the size effects laws was shown to be rather fickle. By examining the various size effect laws in Figure 2 outside of the data range for which they were calibrated, a large difference is seen. This difference is imposed by the mathematical structure of the laws which have been constructed on the basis of specific beliefs. If a larger size range than what has been tested were to become available then all the size effect laws would again span this larger size range in the same fashion as Figure 2a with the same order of disagreement in the extrapolated region. Future research on this topic does not lie within the proposition of various curve fit or size effect laws such as those just examined. There is a clear need for a quantitative basis to the predicted size effects. The latter basis will reside with approaches reflective of the true material behavior.

## 6 Acknowledgements

Phases I & II of this study were supported in part by a joint-industry-agency project (JIAP) initiated (Denis Blanchet) and managed (Kurt Kennedy) by Canadian Marine Drilling Limited (Canmar), a business unit of the Amoco Canada Petroleum Company specializing in arctic offshore drilling and marine activities. Funding for the JIAP was provided by Amoco, Canmar (Canada), Mobil, National Energy Board (Canada), Texaco (Phase I), Minerals Management Service and the Office of Naval Research (ONR). The latter support was provided as part of ONR's Sea Ice Mechanics Accelerated Research Initiative [Grants N00014-90-J-1360 & N00014-93-1-0714].

## 7 References

- Adamson, R. M., Dempsey, J. P., Mulmule, S. V., DeFranco, S. J., and Xie, Y. (1995) Large-Scale In-Situ Ice Experiments, Part I: Experimental Aspects, in **ICE MECHANICS-1995**, ASME Joint Applied Mechanics and Materials Summer Conference, AMD - MD '95, University of California, Los Angeles, June 28-30, 1995.
- Bazant, Z. P. (1984) Size effect in Blunt Fracture: Concrete, Rock, Metal, in **ASCE Journal of Engineering Mechanics**, Vol. 110, 518-535.
- Carpinteri, A., Chiaia, B., and Ferro, G. (1993) Multifractal Scaling Law for the Nominal Strength Variation of Concrete, in **Size Effect in Concrete Structures, Proceedings of the Japan Concrete Institute International Workshop, Sendai, Japan** (eds Mihashi, H., Okamura, H., and Bazant, Z. P.), 193-205.
- DeFranco, S.J. and Dempsey, J.P. (1994) Crack Propagation and Fracture Resistance in Saline Ice, in **Journal of Glaciology**, Vol. 40, 451-462.
- Dempsey, J.P. (1991) The Fracture Toughness of Ice, in **Ice Structure Interaction** (S. J. Jones, R. F. McKenna, J. Tillotson, and I. J. Jordaan), Springer-Verlag, Berlin Heidelberg, 109-145.
- Dempsey, J.P., Wei, Y., and DeFranco, S.J. (1992) Notch Sensitivity and Brittleness in Fracture Testing of S2 Columnar Freshwater Ice, in **International Journal of Fracture** **53**, 101-120.
- Dempsey, J.P., Adamson, R.M., and DeFranco, S.J. (1995) Fracture Analysis of Base-Edge-Cracked Reverse-Tapered Plates, in **International Journal of Fracture** (in press).
- Kim, J. K., Park, Y. D., and Eo, S. H. (1993) Size Effect in Concrete Specimen with Dissimilar Initial Cracks, in **Size Effect in Concrete Structures, Proceedings of the Japan Concrete Institute International Workshop, Sendai, Japan** (eds Mihashi, H., Okamura, H., and Bazant, Z. P.), 181-192.
- Mulmule, S.V., Dempsey, J.P., and Adamson, R.M. (1995) Large-Scale In-Situ Ice Fracture Experiments - Part II: Modeling Efforts, in **ICE MECHANICS-1995**, ASME Joint Applied Mechanics and Materials Summer Conference, AMD - MD '95, University of California, Los Angeles, June 28-30, 1995.